Chinese Chemical Letters 36 (2025) 110317

Contents lists available at ScienceDirect

Chinese Chemical Letters

journal homepage: www.elsevier.com/locate/cclet

PD-L1/SHP2 dual PROTACs inhibit melanoma by enhancing T-cell killing activity

Yang Liu[a,1], Jing Liang[a,1], Mengzhu Zheng[c,1], Haoze Song[a], Lixia Chen[a,*], Hua Li[a,b,*]

[a] Key Laboratory of Structure-Based Drug Design & Discovery, Wuya College of Innovation, Ministry of Education, Shenyang Pharmaceutical University, Shenyang 110016, China
[b] Fujian Key Laboratory of Chinese Materia Medica, Institute of Structural Pharmacology & TCM Chemical Biology, College of Pharmacy, Fujian University of Traditional Chinese Medicine, Fuzhou 350122, China
[c] School of Pharmacy, Tongji Medical College, Huazhong University of Science and Technology, Wuhan 430030, China

ARTICLE INFO

Article history:
Received 23 April 2024
Revised 3 August 2024
Accepted 5 August 2024
Available online 6 August 2024

Keywords:
PD-L1
SHP2
PROTACs
Dual PROTACs
Degrader
Melanoma

ABSTRACT

Programmed cell death protein 1/programmed cell death 1 ligand 1(PD-1/PD-L1) protein-protein interaction represents an appealing target for cancer therapy. Several antibody drugs have been developed to target this interaction, but they are less effective in the treatment of melanoma. To overcome the limitations, the first proteolysis-targeting chimeric (PROTAC) small molecules simultaneously targeting PD-L1 and Src homology phosphotyrosyl phosphatase 2 (SHP2) were designed. By employment of PD-1/PD-L1 inhibitors BMS01 or BMS-37, SHP2 inhibitor SHP099 and E3 ligase ligands, a series of potent PD-L1 and SHP2 dual PROTACs were synthesized. The most promising compounds **BS-7C-V2** and **BS327V2** efficiently induced PD-L1 and SHP2 degradation and demonstrated significantly improved immune potency in B16-F10 and A375 cell lines. More importantly, the efficacy of **BS-7C-V2** and **BS327V2** in a B16-F10 transplanted mouse model was further evaluated based on their degradation ability *in vivo*. Taken together, our work qualifies the new dual PROTACs as a potent degrader of PD-L1 and SHP2. The biological and mechanism investigations with **BS-7C-V2** and **BS327V2** prove that dual PROTACs can play an anti-tumor role *in vivo* and *in vitro*, and can provide a new therapeutic strategy for melanoma.

Immunotherapy and targeted therapy are the main non-surgical treatment methods for melanoma [1]. Due to its ability to persistently control the progression of melanoma and achieve a better prognosis, immune checkpoint blockade therapy has attracted much attention [2]. At present, multiple programmed cell death protein 1/programmed cell death 1 ligand 1 (PD-1/PD-L1) antibody drugs have been used for the treatment of melanoma [1]. However, studies have shown that the overall response rate to PD-L1 antibody drug therapy is not high for melanoma (26%), non-small cell lung cancer (21%), and renal cell carcinoma (13%) [3,4]. To improve the treatment response rate of PD-1/PD-L1 blockade therapy, many drug development institutions have explored the potential of combination therapy strategies in clinical trials. However, the combination therapy strategy not only improves treatment efficacy and response rate but also increases the incidence of treatment-related serious adverse events [5]. Therefore, it is urgently needed to propose more reasonable combination therapy strategies.

Src homology phosphotyrosyl phosphatase 2 (SHP2) is the first reported oncogenic tyrosine phosphatase, encoded by the *PTPN11* and widely expressed in various tissues and cells [6]. Research has shown that the SHP2 inhibitor SHP099 can reduce tumor burden by restoring or enhancing $CD8^+$ T-cell-mediated anti-tumor immunity. In addition, this study also demonstrated that the combination of SHP099 and PD-1 antibody can block the transmission of inhibitory immune signaling and demonstrate a synergistic effect in a colon cancer mouse model [7]. Between 2021 and 2024, Jacobio Pharmaceuticals Co., Limited and Novartis Pharmaceuticals respectively launched phase I/II clinical trials for the combination of PD-1 antibodies and SHP2 small molecule inhibitors [8]. The above research results suggest that the combination of SHP2 and PD-1/PD-L1 is of great value for cancer treatment.

Inspired by bispecific antibody drugs, our research group was the first to propose the concept of dual proteolysis-targeting chimeric (dual PROTAC), designing and synthesizing a dual-targeted degradation agent that can simultaneously degrade epidermal growth factor receptor (EGFR) and poly ADP-ribose polymerase (PARP). This technology simultaneously absorbs the advantages of PROTAC and dual-targeted drugs, while maintaining

* Corresponding authors.
E-mail addresses: syzyclx@163.com (L. Chen), lihua@fjtcm.edu.cn (H. Li).
[1] These authors contributed equally to this work.

https://doi.org/10.1016/j.cclet.2024.110317
1001-8417/

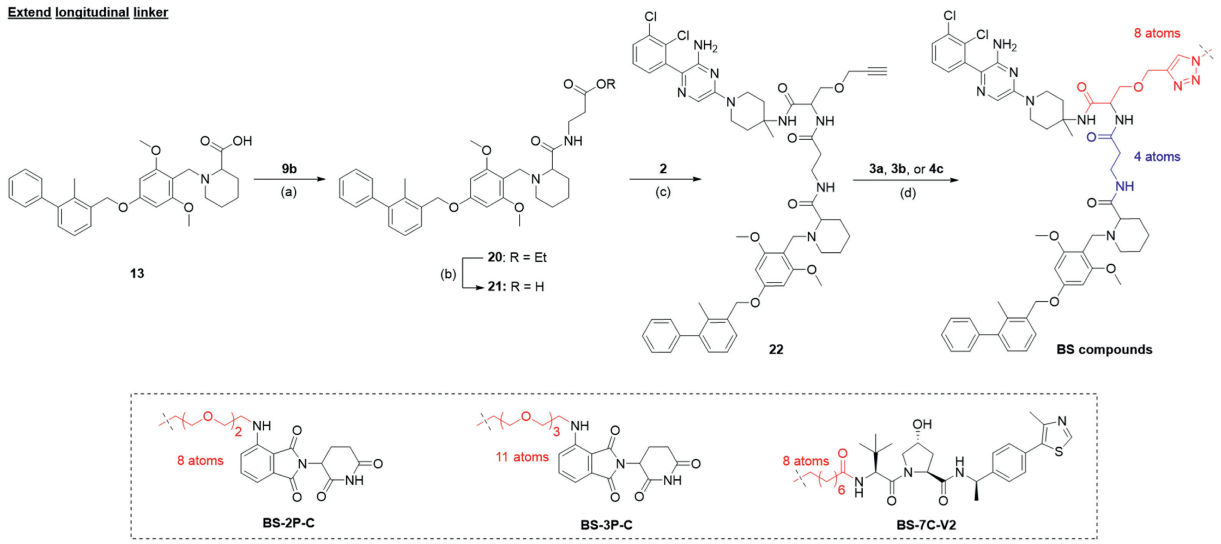

Scheme 1. The synthesis of the BS series of dual PROTACs. Reagents and conditions: (a) HATU, DIPEA, DMF, r.t.; (b) NaOH, $CH_3OH/H_2O = 4:1$, r.t.; (c) EDCI, HOBt, DIPEA, DCM, 0 °C to r.t.; (d) $CuSO_4$, L-sodium ascorbate, $THF/H_2O = 1:1$, r.t.

the properties of small molecule drugs [9]. Given that immune checkpoint blockade therapy for melanoma requires a more rational combination therapy strategy and the enormous potential of PD-1/PD-L1 and SHP2 combination therapy, this study used dual PROTAC technology to design and synthesize PD-L1/SHP2 dual PROTACs to clarify the synergistic therapeutic effect of targeting PD-L1 and SHP2 on melanoma. This study is a supplement to the direct combination strategy of PD-L1 and SHP2, which may provide a promising new treatment option for melanoma from the field of target protein degradation drug development.

The rational design of PD-L1/SHP2 dual PROTACs is mainly based on the SHP2 PROTAC and PD-L1 PROTAC reported by our research group. The SHP2 degrader SP4 with pomalidomide as the CRBN-E3 ligase ligand, displays the best SHP2 degradation activity. Compared to SP4, SP3 exhibits a similar activity [10]. In addition, the SHP2-degrading agent D26 base on VHL-E3 ligase ligand was reported by Wang's group, and 30 nmol/L D26 can cause complete degradation of SHP2 in KYSE520 cells [11]. PD-L1 PROTACs were designed with biphenyl compounds as PD-L1 ligands, which have gradually attracted the attention of many researchers in recent years. However, different biphenyl PD-L1 ligands have a great impact on the degradation activity of the final compounds. Successful cases include BMS-37-C3 and P22 (Fig. S1 in Supporting information) [12,13].

Subsequently, based on the workflow of dual PROTAC technology [9], SHP099 was selected as the SHP2 ligand, while BMS-37 and BMS01 (PD-L1 inhibitors, which have not been used in PD-L1 degradation agent research) [14] were chosen as PD-L1 ligands, and a star-type linker with serine as the basic structure was used for the rational design of SHP2/PD-L1 dual PROTACs. Inspired by successful SHP2 degraders, we determined that the transverse length X of the dual PROTAC molecule is 19 or 16 atoms (Fig. S2A in Supporting information).

In step 1, we fixed X and connected PD-L1 ligands directly to a star-type linker (longitudinal length $Y = 0$ atoms) and designed and synthesized six final compounds (Fig. S2B and Scheme S1 in Supporting information). Western blot results showed that the dual-targeted degradation activities of the above six compounds were low, with no discernible change in the expression of PD-L1 or SHP2 (Fig. S3 in Supporting information). We speculated that the SHP2 ligand and PD-L1 ligand are so close in these compounds that there is a large spatial steric resistance between them. Thus, they cannot bind to their respective target proteins. According to previous literature, the rigid structure of the PD-L1 degrader is beneficial for degradation [13]. In step 2, we extended the longitudinal length Y of the BSS series of compounds to determine whether the above hypothesis was true.

In step 2, we fixed X and extended the longitudinal linker Y to 4 atoms (Fig. S2C in Supporting information). This plan was achieved by introducing ethyl 3-aminopropanoate to the carboxyl group of the PD-L1 ligand BMS01, and three compounds were synthesized (Scheme 1). **BS-3P-C** showed modest degradation at 10 μmol/L (the half-maximal degradation concentration (DC_{50}) of SHP2 is 2.85 μmol/L and PD-L1 $DC_{50} = 0.82$ μmol/L in A375 cells; SHP2 $DC_{50} = 11.82$ μmol/L and PD-L1 $DC_{50} = 3.20$ μmol/L in B16-F10 cells). **BS-7C-V2** had the most potent degradation efficiency in a concentration-dependent manner, starting to degrade at 1 μmol/L and reaching a peak at 10 μmol/L with a degradation rate of more than 90% (Figs. 1A and B, Fig. S4 in Supporting information) (SHP2 $DC_{50} = 0.56$ μmol/L and PD-L1 $DC_{50} = 0.37$ μmol/L in A375 cells; SHP2 $DC_{50} = 0.12$ μmol/L and PD-L1 $DC_{50} = 2.19$ μmol/L in B16-F10 cells). This result proves the feasibility of this reasonable design and demonstrates that steric hindrance has a great influence on the degradation activity of dual PROTACs.

To obtain compounds with better activity, we optimized **BS-3P-C** and **BS-7C-V2** (Figs. S2D and E in Supporting information). Since **BS-2P-C** ($X = 16$ atoms) did not achieve dual-targeted degradation, we mainly extended the transverse length X of **BS-3P-C** ($X = 19$ atoms). Four compounds (**BS-4P-C**, **BS123C**, **BS223C**, and **BS323C**) were synthesized by introducing linkers of different lengths to adjust X to 22, 22, 23, or 24 atoms, respectively (Scheme S2 in Supporting information). For the optimization of **BS-7C-V2**, we shortened or extended the linker, adjusted X to 12, 14, 19, 20, or 21 atoms, and synthesized five compounds (**BS-3C-V2**, **BS-5C-V2**, **BS127V2**, **BS227V2** and **BS327V2**). **BS-7C-V1** was synthesized by replacing VHL-E3 ligase ligands (Scheme S3 in Supporting information). The dual PROTACs recruited CRBN without degrading both the PD-L1 and SHP2 proteins (Fig. S5 in Supporting information), while those recruiting VHL degraded both PD-L1 and SHP2, and the degradation became more pronounced with increasing linker concentration. **BS327V2** exhibited comparable or even better PD-L1/SHP2 degradation activity than **BS-7C-V2** (SHP2 $DC_{50} = 0.42$ μmol/L and PD-L1 $DC_{50} = 0.015$ μmol/L in A375 cells; SHP2 $DC_{50} = 5.40$ μmol/L and PD-L1 $DC_{50} = 0.11$ μmol/L in B16-F10 cells) (Figs. 1C and D, Fig. S6 in Supporting information). In addition, the degradation activity of **BS-7C-V2** was better than that of

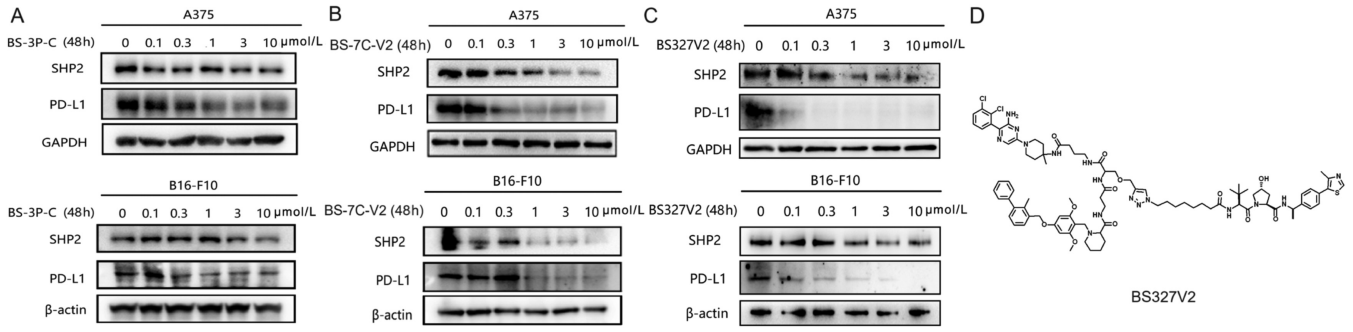

Fig. 1. The PD-L1 and SHP2 level in A375 and B16-F10 cells after treatment with **BS-3P-C** (A), **BS-7C-V2** (B) and **BS327V2** (C) for 48 h. (D) The structure of **BS327V2**. GAPDH, glyceraldehyde-3-phosphate dehydrogenase.

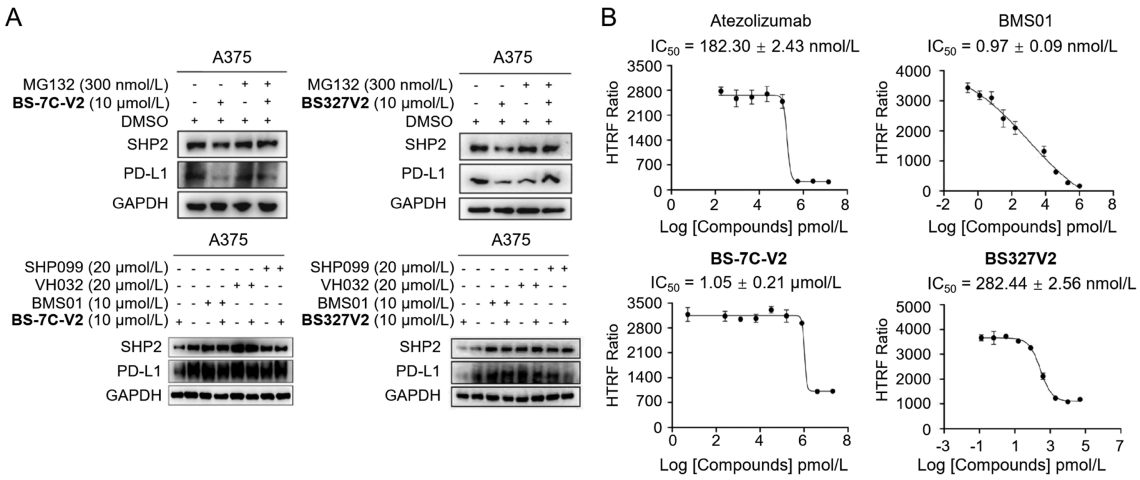

Fig. 2. The verification of degradation mechanism and the determination of inhibitory activity of compounds on PD-1/PD-L1 interactions. (A) Investigation of the mechanism of PD-L1/SHP2 degradation by **BS-7C-V2** or **BS327V2**. (B) The ability of Atezolizumab, BMS01, **BS-7C-V2** and **BS327V2** to inhibit the interaction between PD-1 and PD-L1. Data are presented as mean ± standard deviation (SD) ($n = 3$).

BS-7C-V1 (Figs. S6 and S7 in Supporting information). Thus, **BS-7C-V2** and **BS327V2** were selected for subsequent research.

In A375 or B16-F10 cells, proteasome inhibitor MG132 can reverse the simultaneous degradation of PD-L1/SHP2 mediated by **BS-7C-V2** or **BS327V2** (Fig. 2A). Due to the formation of the ternary complex (Target Protein-PROTAC-E3 ligase) being a key step in the degradation activity of PROTAC molecules, the ligand competition method was used to further validate the degradation mechanisms of **BS-7C-V2** and **BS327V2**. The results showed that PD-L1 ligand BMS01 had no significant effect on the protein expression level of PD-L1, but could inhibit the degradation activity of **BS-7C-V2** and **BS327V2**, indicating that BMS01 inhibits the formation of ternary complexes by competitively binding to PD-L1, thereby reducing the degradation activity of dual PROTACs (Fig. 2A). SHP2 ligand SHP099 displayed a similar effect on **BS-7C-V2** and **BS327V2** (Fig. 2A). In addition, the effect of VHL-E3 ligase ligand VH032 on the degradation activity of **BS-7C-V2** and **BS327V2** was also tested in this section, and the results showed that VH032 can also hinder the degradation effect of **BS-7C-V2** and **BS327V2** (Fig. 2A). In summary, the degradation of PD-L1 and SHP2 mediated by **BS-7C-V2** and **BS327V2** depends on the ubiquitin-proteasome pathway.

The cytotoxicity of all compounds on A375 and B16-F10 cells was evaluated using the cell counting kit-8 (CCK-8) method. The results showed that most compounds did not exhibit excellent cytotoxic activity against A375 and B16-F10 cells (Table S1 in Supporting information), indicating that the simultaneous degradation of PD-L1 and SHP2 induced by **BS-7C-V2** and **BS327V2** was not caused by the cytotoxic activity of the compounds.

The activities of the compounds as inhibitors of PD-1/PD-L1 interactions were evaluated using the well-established HTRF assay, and the inhibitory activities are presented as the half maximal inhibitory concentration (IC_{50}) values [15]. Therefore, we tested prescreened **BS-7C-V2** and **BS327V2**, and found that their IC_{50} values against PD-1/PD-L1 were 1.05 ± 0.21 μmol/L and 282.44 ± 2.56 nmol/L, respectively (Fig. 2B). At the same time, the PD-L1 monoclonal antibody atezolizumab was selected as a positive control with an IC_{50} value of 182.30 ± 2.43 nmol/L (Fig. 2B). In addition, the PD-L1/PD-L1 inhibitory activity of BMS01, the PD-L1 ligand used for the synthesis of PD-L1 from **BS-7C-V2** and **BS327V2**, was also tested, with an IC_{50} value of 0.97 ± 0.09 nmol/L (Fig. 2B). The above results indicate that **BS-7C-V2** and **BS327V2** can significantly inhibit the interaction between PD-1/PD-L1.

The above experiments showed that the synthesized dual PROTACs could indeed reduce the levels of PD-L1 and SHP2 proteins at the cellular level. However, the unique capabilities of PD-L1/SHP2 dual PROTACs also need to be reflected in their ability to improve the efficiency of T-cells. Therefore, we established a T-cell co-culture model to detect the killing effect of T-cells on tumor cells. The morphology of activated T-cells after stimulation is shown in Fig. 3A. When the ratio of tumor cells to T-cells was 1:3 in co-culture, T-cells killed approximately 50% of the tumor cells (Fig. 3B). Therefore, we used this ratio in subsequent co-culture experiments. When combined with T-cells, **BS-7C-V2** and **BS327V2** significantly increased the killing activity of T-cells against A375 cells (Figs. 3C and D). As shown in Figs. 3D and E, the anti-tumor immune effect of the synthesized dual PROTACs was comparable to that of atezolizumab, a monoclonal antibody against PD-L1.

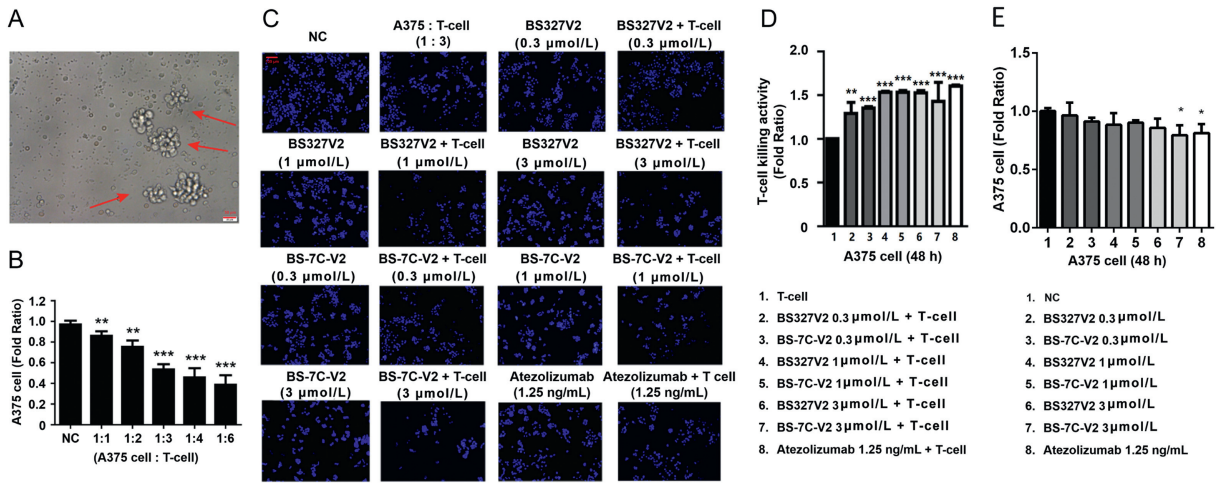

Fig. 3. The killing activity of the **BS327V2** and **BS-7C-V2** was evaluated by a T-cell co-culture assay. (A) Microscopic view of stimulated T-cells after primary culture. Scale bar: 50 μm. (B) Study of the efficiency and target ratio of tumor cell and T-cell co-culture. Tumor cells and T-cells were co-cultured at ratios of 1:1, 1:2, 1:3, 1:4, and 1:6 for 2 days, and then fixed, stained and photographed were counted. Each data point represents three independent experiments. $^{**}P < 0.01$, $^{***}P < 0.001$ *vs.* negative control (NC) group. (C) Cytotoxic effect of **BS327V2** and **BS-7C-V2** on A375 cells after co-culture with T-cells. The cells were stained with 4′,6-diamidino-2′-phenylindole (DAPI). Scale bar: 100 μm. (D) Statistical graph of the T-cell killing activity of **BS327V2**, **BS-7C-V2**, and Atezolizumab. Each data point represents three independent experiments. $^{**}P < 0.01$, $^{***}P < 0.001$ *vs.* T-cell group. (E) Statistical graph of the cytotoxic effects of **BS-7C-V2**, **BS327V2**, and Atezolizumab on A375 cells. Each data point represents three independent experiments. $^{*}P < 0.05$ *vs.* NC group. Data are presented as mean ± SD ($n = 3$).

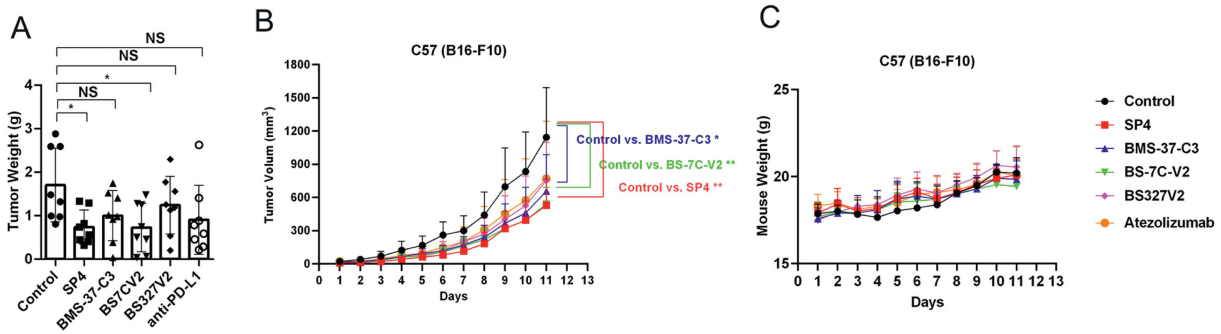

Fig. 4. Evaluation of the efficacy of **BS-7C-V2** and **BS327V2** in the B16-F10 tumor model. (A) Differences in B16-F10 tumor weight after 11 days of treatment with SP4, **BMS-37-C3**, **BS-7C-V2**, **BS327V2** and Atezolizumab. $n = 8$ mice per group. (B) Compounds had no effect on mouse body weight. (C) Final tumor size of each group. NS, not significant. $^{*}P < 0.05$, $^{**}P < 0.01$ *vs.* control group. Data are presented as mean ± SD ($n = 3$).

The *in vivo* anti-tumor activity of **BS-7C-V2** and **BS327V2** was evaluated in a B16-F10 transplanted tumor mouse model. All protocols were approved by the Animal Experimentation Committee of Tongji Medical College, Huazhong University of Science and Technology (IACUC Number: 3408). The experimental results showed that SHP2 PROTAC SP4 can significantly inhibit tumor growth, with a tumor growth inhibition rate (TGI) of 53.65%. The TGI of PD-L1 PROTAC BMS-37-C3 and Atezolizumab were 42.57% and 32.60%, respectively (Fig. 4A). In contrast, the tumor growth inhibitory activity of **BS-7C-V2** is better than BMS-37-C3 and Atezolizumab, with a TGI of 52.75%. In addition, no significant weight changes or significant adverse reactions were observed during the experiment (Figs. 4B and C). The above results indicated that SP4, BMS-37-C3, **BS-7C-V2** and **BS327V2** all exhibit certain anti-tumor activity against melanoma *in vivo*.

In addition, we also weighed the tumors and spleens of the mice to further validate our previous findings (Fig. S8A in Supporting information). After the mice were sacrificed, two tumor samples from the six treatment groups were randomly collected and probed for PD-L1 and SHP2 expression. As expected, all dual PROTACs were capable of inducing the degradation of the PD-L1 and SHP2 proteins, but no significant changes in the vehicle control group or positive control group were observed (Fig. S8B in Supporting information). Overall, these findings are consistent with the *in vitro* experiments. To further examine the effect of drugs on tumor immunity in mice, we randomly selected three samples from each group for flow-through assays. The results showed that both the antibody and drug treatments promoted tumor immunity, but the effect in the dual PROTAC group was greater than that in the other groups (Fig. S8C in Supporting information).

In recent years, some PD-1/PD-L1 inhibitors have shown definite efficacy in the treatment of advanced malignant melanoma [16,17]. In addition, many studies have shown that PD-L1 combined with other targets, such as PD-1, histone deacetylase 2 (HDAC2), and Toll-like receptor 1/2 (TLR1/2), has great research and application potential in the treatment of melanoma [18–20]. However, in the case of monotherapy or combination therapy, the majority of studies are based on PD-L1 or PD-1 antibody drugs, showing some limitations in their clinical application. The combined utilization of multiple drugs may also cause toxic stacking. To address the above issues, we integrated the concepts of cancer immunotherapy, dual targeting, and PROTAC, replacing the combined application of these two drugs with a small-molecule degrader. We also utilized the catalytic properties of PROTACs to reduce toxic side effects and synergistically increase anti-cancer effects.

The combination of PD-L1 and SHP2 is effective and reasonable in many cancer treatments [21,22], but its therapeutic potential in melanoma needs to be studied. In this study, we described the design, synthesis, optimization, and activity evaluation of dual PD-L1/SHP2 PROTACs. This study successfully achieved the simul-

taneous degradation of PD-L1 and SHP2 in A375 and B16-F10 cell lines, further enriching the application examples of the dual PROTAC concept and providing alternative small molecule drugs for the treatment of melanoma based on immune checkpoint blocking (ICB) therapy. Moreover, studies have shown the great potential of the combination of PD-L1 and SHP2 for the treatment of melanoma.

One study showed that the degradation of PD-L1 can reprogram the inhibitory tumor microenvironment [23], and our study further confirmed this conclusion. PD-L1/SHP2 dual PROTACs had little effect on the survival rate of the two kinds of melanoma cells, but **BS-7C-V2** enhanced the ability of the T-cells to kill the melanoma cells. The above results suggest that **BS-7C-V2** may exert anticancer effects by regulating the immune microenvironment. In addition, **BS-7C-V2** showed better tumor growth inhibitory activity than PD-L1 monoclonal antibody *in vivo*, and the impact on mouse body weight was equivalent. PD-L1/SHP2 dual PROTACs indeed achieved the objective of increasing anti-tumor activity and reducing toxic side effects. This will overcome the limitations of existing therapeutic drugs and will also provide a new strategy for the treatment of melanoma.

In this study, nineteen SHP2/PD-L1 dual PROTACs were synthesized through reasonable design, among which **BS-7C-V2** is the most promising compound. **BS-7C-V2** can simultaneously induce protein degradation of PD-L1 and SHP2 in a time-dependent manner and exert antimelanoma effects by enhancing the killing ability of T-cells. In addition, **BS-7C-V2** showed better anti-tumor activity than the PD-L1 monoclonal antibody *in vivo*. To further improve the activity of PD-L1/SHP2, optimization will be carried out for linker types and E3 ligands [24,25]. This study clarifies the synergistic effect of SHP2 and PD-L1 in the treatment of melanoma and provides a new approach for the treatment of melanoma.

Declaration of competing interest

The authors declare that they have no known competing financial interests or personal relationships that could have appeared to influence the work reported in this paper.

CRediT authorship contribution statement

Yang Liu: Writing – original draft. **Jing Liang:** Writing – original draft. **Mengzhu Zheng:** Writing – original draft. **Haoze Song:** Visualization. **Lixia Chen:** Writing – review & editing, Supervision, Funding acquisition, Conceptualization. **Hua Li:** Writing – review & editing, Supervision, Conceptualization.

Acknowledgments

The authors thank the National Natural Science Foundation of China (NSFC, No. 82141216), Chunhui Program-Cooperative Research Project of the Ministry of Education, Project of Frontier Technology Platform for Research Projects of Liaoning Provincial Department of Education in 2024, and Shenyang Young and Middle-aged Innovative Talents Support Program (No. RC210446) for financial supports. And we acknowledged the support from National-Local Joint Engineering Research Center for Molecular Biotechnology of Fujian & Taiwan TCM at Fujian University of Traditional Chinese Medicine.

Supplementary materials

Supplementary material associated with this article can be found, in the online version, at doi:10.1016/j.cclet.2024.110317.

References

[1] B.D. Curti, M.B. Faries, New Engl. J. Med. 384 (2021) 2229–2240.
[2] J.D. Wolchok, V. Chiarion-Sileni, R. Gonzalez, et al., J. Clin. Oncol. 40 (2022) 127–137.
[3] M. Sznol, Cancer J. 20 (2014) 290–295.
[4] R.S. Herbst, J.C. Soria, M. Kowanetz, et al., Nature 515 (2014) 563–567.
[5] X. Zhou, Z. Yao, H. Bai, et al., Lancet Oncol. 22 (2021) 1265–1274.
[6] D. Imbody, K. Arce, H.S. Solanki, et al., J. Thorac. Oncol. 19 (2024) 18–24.
[7] M. Zhao, W. Guo, Y. Wu, et al., Acta Pharm. Sin. B 9 (2019) 304–315.
[8] M. Wu, Q. Huang, Y. Xie, et al., J. Hematol. Oncol. 15 (2022) 24.
[9] M. Zheng, J. Huo, X Gu, et al., J. Med. Chem. 64 (2021) 7839–7852.
[10] M. Zheng, Y. Liu, C. Wu, et al., Bioorg. Chem. 110 (2021) 104788.
[11] M. Wang, J. Lu, M. Wang, et al., J. Med. Chem. 63 (2020) 7510–7528.
[12] Y. Liu, M. Zheng, Z. Ma, et al., Chin. Chem. Lett. 34 (2023) 107762.
[13] B. Cheng, Y. Ren, H. Cao, et al., Eur. J. Med. Chem. 199 (2020) 112377.
[14] Y. Zhao, Y. Jia, T. Shi, et al., Carcinogenesis 40 (2019) 1132–1141.
[15] Z. Yang, Z. Liu, C. Xu, et al., Bioorg. Chem. 139 (2023) 106740.
[16] J. Weber, M. Mandala, M. Del Vecchio, et al., N. Engl. J. Med. 377 (2017) 1824–1835.
[17] J. Brahmer, S. Tykodi, L. Chow, et al., N. Engl. J. Med. 366 (2012) 2455–2465.
[18] G. Hartley, L. Chow, D. Ammons, et al., Cancer Immunol. Res. 6 (2018) 1260–1273.
[19] J. Yu, A. Zhuang, X. Gu, et al., Cell Discov. 9 (2023) 33.
[20] Y. Wang, L. Su, M. Morin, et al., Proc. Natl. Acad. Sci. U. S. A. 115 (2018) E8698–E8706.
[21] A. Drilon, M. Sharma, M. Johnson, et al., Cancer Discov. 13 (2023) 1789–1801.
[22] D. Chen, H. Barsoumian, L. Yang, et al., Cancer Immunol. Res. 8 (2020) 883–894.
[23] W. Su, M. Tan, Z. Wang, et al., Angew. Chem. Int. Ed. 62 (2023) e202218128.
[24] X. Han, W. Wei, Y. Sun, Acta Mate. Med. 1 (2022) 244–259.
[25] Y. Jing, C. Zuo, Y. Du, et al., Chin. Chem. Lett. 34 (2023) 107781.